

1 Integrating multiple surveys to account for changing ocean conditions
2 and spatial distribution shifts of black sea bass

3 Alexander Hansell¹, Kiersten Curti¹

4 1) NOAA Northeast Fisheries Science Center, Woods Hole, MA, USA

5
6 **Abstract:**

7 In US waters of the Atlantic, black sea bass support important commercial and recreational fisheries. The
8 northern stock ranges from the Gulf of Maine to Cape Hatteras, North Carolina. It is well documented
9 that ocean conditions are changing in this region of the Atlantic and it is hypothesized that black sea
10 bass distribution and productivity could be affected by climate change. The current stock assessment
11 does not account for environmental effects and accounts for spatial dynamics by splitting the stock into
12 two regions at Hudson canyon: the north and south. Despite this spatial split, the assessment still has
13 poor retrospective patterns, which could be caused by numerous factors including changing ocean
14 conditions or spatio-temporal dynamics. Here, we fit a series of spatio-temporal models to 10 seasonal
15 trawls surveys in the stock region. Seasonal models were used to produce both aggregated and age-
16 based distribution and abundance estimates. Model selection indicated that for all models, bottom
17 temperature was an important covariate influencing fish density, and survey influenced catchability.
18 Model results suggest that black sea bass center of gravity has shifted northeast in the South and that
19 their range has expanded poleward. Age-based estimates in the spring suggest that all ages have shifted
20 northeast and in both seasons, age-1 fish have increased their range. Results suggest that relative
21 abundance has increased in the North and remained stable in the South. Ultimately, results characterize
22 changes in spatial distribution and provide indices and age-compositions that are robust to spatio-
23 temporal changes for consideration in stock assessment.

24

25 Keywords: Spatio-temporal, species distribution, climate change, fisheries independent

26

27

28 **Introduction:**

29 In United States waters of the northwest Atlantic, fisheries are an important cultural and economic part
30 of society. Because of this, many governmental agencies, both state and federal, have devoted
31 resources to conducting annual scientific surveys in the region. A primary purpose of these surveys is to
32 monitor fish abundance, distribution, and provide inputs to population assessments. An assumption of
33 using survey estimates in stock assessment is that trends are directly proportional to population
34 abundance. Thus, ideally surveys are designed to have consistent sampling that are representative of
35 populations, in space and time, and can be compared across years.

36 Even the most well designed surveys are often subject to sampling changes over time (e.g., weather,
37 mechanical issues, changes in survey vessel, Covid -19) that cannot be avoided. Further, many fish have
38 complicated spatio-temporal dynamics that are linked to the environment, while surveys typically have
39 limited temporal sampling windows and for smaller surveys, limited spatial footprints. In the northwest
40 Atlantic, it is well documented that ocean conditions are changing causing spatio-temporal changes in
41 species distribution and abundance (Nye et al., 2009; Pinsky et al. 2013). Failure to account for these
42 changes can lead to inaccurate perception of abundance trends and poor understanding of population
43 dynamics (Wilberg et al. 2010, Link et al 2011).

44 Spatio-temporal models can estimate changes in population density over time at multiple locations
45 while accounting for environmental variables and unknown processes. These models are being used
46 frequently in climate, habitat and stock assessments (Thorson, 2019). Spatio-temporal frameworks are
47 especially useful for estimating center of gravity because it allows for multiple explanatory covariates to
48 be explored in the same framework (Perretti and Thorson, 2019). These models can then incorporate
49 the potential drivers and spatial changes into indices of abundance and composition data for input into
50 stock assessment (O'Leary et al. 2020). Spatio-temporal models can also be used to integrate multiple
51 surveys into a single index of abundance (O'Leary et al. 2022). A joint index can help reconcile noisy or
52 conflicting indices, account for changes in availability and simplify inputs to stock assessment, allowing
53 for improved assessment performance (Conn, 2010). Additionally, using the results from spatio-
54 temporal models has been demonstrated to yield more precise/accurate indices of abundance (Shelton
55 et al. 2014). Fitting assessments to spatio-temporal standardized indices can also lead to less
56 retrospective bias and outperform assessments with design-based indices (Cao et al. 2017).

57 Black sea bass are a coastal species that supports important commercial and recreational fisheries. In
58 the western Atlantic, they are assessed as two separate populations: the northern stock and South
59 Atlantic stock. The northern stock is further split into two regions: North and South, with the dividing
60 line being Hudson Canyon. The stock was split into two regions to account for spatial dynamics and
61 improve model diagnostics (NEFSC 2017). Since the last major benchmark in 2017, the stock assessment
62 is fit to 17 indices of abundance, including 14 trawl surveys. Nine of the indices are produced from
63 inshore trawl surveys and have small spatial footprints, while five of the indices are from the Northeast
64 Fisheries Science Center bottom trawl survey, which has a large spatial footprint.

65 Black sea bass make seasonal migrations, moving inshore in the spring and offshore in the fall (Moser
66 and Shepherd, 2009). Black sea bass distribution has been linked to warming waters on the Northeast
67 US Shelf (Bell et al. 2016) and it is hypothesized that black sea bass are especially susceptible to climate
68 change with likely shifts in distribution and productivity due to warming water temperatures (Hare et al.,
69 2015). Current assessments have major retrospective patterns and account for spatial dynamics by
70 splitting the stock into two assessments. Neither assessment directly accounts for climate effects (NEFSC
71 2022). Incorporating spatio-temporal dynamics or climate effects could potentially help to improve
72 retrospective patterns (Cao et al. 2017; Mazur et al. 2023). Thus a major research recommendation for
73 this species is to better understand how changes in the environment are affecting life history and spatial
74 dynamics.

75 Here we fit a series of spatio-temporal models to all available trawl survey data and environmental
76 covariates for the northern stock of black sea bass. Results provide estimates of distribution shifts, area
77 occupied and environmental drives. Further, model output produces a series of joint indices and age
78 composition data that account for these changes and can be directly incorporated into future stock
79 assessments.

80

81 **Methods:**

82 Ten trawl surveys were available (Table 1; Figure 1). All surveys collected information on: catch (kg &
83 numbers), latitude, longitude, time of tow, bottom temperature and depth of tow. Shelf water volume
84 anomaly was matched to survey data because previous studies suggested this covariate might influence
85 over wintering survival (Miller et al. 2016). There was temporal variability in survey sampling so surveys
86 were grouped into two seasons: Spring (January - June) and fall (July - December). Length information

87 was available from all surveys; however, ages were not available for all surveys. Ages were available
 88 from the Northeast Fisheries Science Center Survey and Massachusetts Division of Marine Fisheries
 89 Survey. When ages were not available, lengths were converted to ages using seasonal age-length keys
 90 from the available age information. These are the same age-length keys that are used in the stock
 91 assessment.

92

93 **Model:**

94 Vector Autoregressive Spatio-temporal (VAST) is a delta-model that models the probability of an
 95 encounter and positive catch rate as two separate generalized linear mixed models. Here we use a
 96 binomial distribution for probability of a positive catch and a log-normal distribution for positive catch.

97 Probability of a black sea bass observation:

$$98 \quad \text{logit}^{-1}(P_{1,i}) = \beta_1(t_i, c_i) + \omega_1(s_i, c_i) + \varepsilon_1(s_i, c_i, t_i) + \sum_{j=1}^{n_j} \lambda_1(j, c_i)x(j, s_i, t_i)Q(i, k_1)$$

99 Black sea bass catch on positive trips:

$$100 \quad \log(P_{2,i}) = \beta_2(t_i, c_i) + \omega_2(s_i, c_i) + \varepsilon_2(s_i, c_i, t_i) + \sum_{j=1}^{n_j} \lambda_2(j, c_i)x(j, s_i, t_i)Q(i, k_2)$$

101 Where P_1 is the probability of positive catch, P_2 is the probability of the catch given the catch is positive,
 102 $\beta(t_i)$ is the intercept for each year t and age-group c and is modeled as a random walk, $\omega(s_i)$ is a time-
 103 invariant spatial autocorrelated variation for knot s and age-group c , $\varepsilon(s_i, c_i, t_i)$ is a time-varying spatial-
 104 temporal autocorrelated variation for knot s and age-group c in year t , $\lambda(j, c_i)$ is the effect of covariate j
 105 on length group c , n_j is the number of covariates and $x(j, s_i, t_i)$ is the value of covariate j in knot s in
 106 year t , $Q(i, k)$ is the fixed effect estimates for catchability, and the integer subscripts denote the model
 107 component (1: presence/absence, 2: non-zero density) for observation i .

108 The spatial processes ($\omega_1(s_i, c_i)$; $\omega_2(s_i, c_i)$) were modeled as Gaussian Markov random fields with
 109 correlation over two spatial dimensions.

$$110 \quad \text{vec}(\Omega_p) \sim \text{GRF}(0, R_p \otimes V_{wp})$$

111 Where Ω_p is a matrix composed of $\omega_2(s_i, c_i)$ at every knot s and length bin c , R_p is correlation between
 112 knots, and V_{wp} is correlation between length bins.

113
$$V_{wp} = L_{wp} L_{wp}^T$$

114 Where L_{wp} is a matrix representing covariance among age bins. The spatial covariance between knots s
 115 and s^* was modeled as a Matern process.

116
$$R_p(s, s^*) = \frac{1}{2^{v-1} \Gamma(v)} (K_p H |s - s^*|)^v K_v(K_p H |s - s^*|)$$

117
 118 Where v is a smoothness parameter that is fixed at 1, K_p controls the distance correlation and reduces
 119 to zero, K_v is a Bessel function and H is a two dimensional anisotropic distance function. The spatio-
 120 temporal processes $(\varepsilon_{1,2}(s_i, c_i, t_i))$ were fit independently for each year, and were modeled with
 121 Gaussian Markov random fields assuming a Matern covariance.

122 In addition to catchability covariate effects, estimated values of the fixed and random effects predicted
 123 local density $(d(s, t))$ for knot s and length-group c in year t .

124
$$d(s, t) = \text{logit}^{-1} \left(\beta_1(t_i, c_i) + \omega_1(s_i, c_i) + \varepsilon_1(s_i, c_i, t_i) \right) \times \exp \left(\beta_2(t_i, c_i) + \omega_2(s_i, c_i) + \varepsilon_2(s_i, c_i, t_i) \right)$$

125
 126 The index of abundance $(B(t))$ is calculated as the sum of the density of each knot using an area
 127 weighted approach:

128
$$B(t) = \sum_{s=1}^{n_s} (a(s) \times d(s, t))$$

129 Where $B(t)$ is the area weighted density for each knot in year t throughout the specific domain and $a(s)$
 130 is the area of knot s . A mesh approach (200 knots) which allows for anisotropy was used to fit the
 131 model. Parameter estimation used Template Model Builder (Kristensen et al. 2016) and the R program
 132 (R Core Team 2020). Model convergence was examined by ensuring the maximum gradient of the
 133 likelihood estimation was less than 0.0001 for all parameters and the Hessian matrix was positive
 134 definite.

135 **Model configuration:**

136 In total, four different models were built: 1) spring annual index; 2) spring age-composition; 3) fall
137 annual index; 4) fall age-composition. For each model we explored: bottom water temperature, depth
138 and shelf water volume as modulates of density or catchability. Survey was also explored as a modulate
139 of catchability. Collinearity of covariates was examined using generalized variance-inflation factor (GVIF)
140 scores. Any covariate with a score greater than three was removed, and the GVIFs were recalculated
141 (Zuur, et al. 2012). Akaike Information Criterion (AIC) scores were used to determine the best-fitting
142 model. If AIC scores were within two units of one another, the most parsimonious model was selected
143 (Burnham and Anderson, 2004).

144 **Results:**

145 For both the spring and fall, AIC supported including survey as a covariate on catchability and bottom
146 water temperature as a modulate of density (Table 2). The age models also included an interaction of
147 survey/age to account for age-specific catchability between the surveys.

148 In general, VAST estimates suggest that black sea bass are more abundant inshore in the fall and more
149 abundant offshore in the spring (Figure 3 & 4). For both seasons, the total proportion of black sea bass
150 caught in the northern region has increased over the time series (Figure 5). The stock-wide center of
151 gravity has shifted northeastward (Figure 6).

152 For both seasons, the center of gravity of black sea bass has generally shifted north in the southern
153 region, while the spatial distribution in the northern region has remained relatively stable (Figure 7 - 8).

154 In contrast, effective area occupied has increased in the northern region in both the fall and spring,
155 while effective area occupied estimates in the south have been variable with no clear trend (Figure 9).

156 Coast-wide age-based estimates suggest that the center of gravity for all ages in the spring has shifted to
157 the northeast (Figure 10). In the fall, coast-wide age estimates show some signs of northeast changes in
158 center of gravity of ages 3-5; however, there is no clear trend (Figure 11). Stock-wide age-based
159 effective area estimates suggest that age-1 fish are using a greater area in both the spring and fall over
160 the course of the time series (Figure 12).

161 Annual index estimates from VAST suggest that abundance in the north has increased in the spring and
162 fall, while abundance has remained relatively stable in the south (Figure 13). In the spring, stock-wide
163 age-based abundance estimates suggest an increase of age-2 and older fish (Figure 14). In the fall, stock-
164 wide age-based abundance estimates show variability for all ages with no clear trend (Figure 15). In the

165 spring, age compositions in each region indicate an expansion in the age structure beginning in
166 approximately 2005. Additionally, spring proportions-at-age in the north show the progression of
167 multiple cohorts through the population, including the 2011 and 2015 year classes. In the south, the
168 progression of the 2011 year class is also evident in the spring age compositions, but it is not as
169 pronounced as in the north. In the fall, age compositions in the north show a similar expansion in age
170 structure and progression of the 2011 cohort as in the spring; however, age compositions in the south
171 are dominated by age-2 fish and do not vary notably over the time series (Figure 16).

172 **Discussion:**

173 For the northern black sea bass stock, spatio-temporal models suggest a range expansion to the north,
174 while fish in the south (between Hudson Canyon and Cape Hatteras) are using the same area but with a
175 northeastward shift in their center of gravity. These results support previous studies that have
176 hypothesized and demonstrated poleward shifts in black sea bass distribution (Hare et al. 2015; Bell et al
177 2016). It is also expected that these poleward shifts could continue into the future due to projected
178 increases in warming and biological demands (Slesinger et al. 2019).

179 Another previous hypothesis about black sea bass is that their productivity in waters north of Hudson
180 Canyon could be increasing due to increased water temperature and improved overwintering survival
181 (Hare et al. 2015; Miller et al. 2016). Results from this study show that age-1 fish in the spring have
182 shifted northeast and are occupying a greater area. Age-1 abundance has increased in the spring but has
183 remained relatively stable since 2000, while age-1 abundance in the fall has been stable throughout the
184 time series. Thus, the results from the spatio-temporal models suggest that changes in spatial
185 distribution are occurring at a faster rate than changes in productivity. However, it is important to note
186 that the surveys used in this study were not specifically designed to capture age-1 black sea bass.
187 Additionally, productivity is one of the most difficult metrics to measure in fisheries science (Maunder
188 and Thorson, 2019).

189 Aggregated black sea bass abundance estimates show increases in the northern region and stable trends
190 in the south. Increasing abundance is not surprising given that black sea bass have a preference for
191 warmer water and their range appears to have expanded in the north. Additionally, higher abundance
192 could be the result of increased overwintering survival in the north due to warmer water temperatures
193 (Miller et al 2016). Increasing abundance is also supported by the last black sea bass stock assessment,
194 which estimated large increases in biomass (NEFSC 2022). Black sea bass abundance could continue to

195 increase in the future. Offshore wind development is rapidly occurring in the northeast US continental
196 shelf with multiple lease areas. These wind farms will increase the amount of structured habitat in the
197 region, which is the preferred habitat for black sea bass (Friedland et al. 2021).

198 The spatio-temporal models used in this study have several assumptions and limitations. VAST is an
199 area-weighted model, thus, it gives weight to surveys that sample a larger area. In this study, that is the
200 spring and fall NEFSC surveys. Thus, the combined index produced by VAST is pre-weighted (by area) to
201 give more leverage to the offshore surveys. Another assumption of this approach is that the trawl
202 surveys all have similar catchabilities. The model does account for differences between the surveys
203 (using a factor); however, this is a relatively simple adjustment that does not directly account for specific
204 differences (e.g., tow time or net width). Additionally, not all of the surveys have the same temporal
205 coverage but they are grouped into spring and fall (Table 1). The inclusion of water temperature, which
206 is correlated with time of year, should help to account for these differences in the model.

207 Another limitation of this study was that some environmental covariates that have been shown to affect
208 black sea bass could not be included in the model. For example, black sea bass abundance has been
209 linked to salinity (Miller et al. 2016). We weren't able to explore salinity in the spatio-temporal models
210 because this covariate was not collected by every survey. However, even if other important explanatory
211 covariates were not included, it is likely that they are correlated with the covariates that were explored.
212 Additionally, the random effects of the model can absorb variation that was not attributed to
213 explanatory variables (Perretti and Thorson, 2019). Despite this, further work should consider exploring
214 additional covariates and their effect on black sea bass abundance and distribution.

215 Despite the limitations, the study also has several advantages. The combined spatial footprints of the
216 different surveys allows for trends representative of the entire stock, while previous studies only
217 focused on offshore waters (Bell et al. 2016; Miller et al. 2016) . The results of the VAST models provide
218 direct inputs for the assessment of the northern stock of black sea bass that can account for changing
219 spatio-temporal dynamics and environmental effects. Another strength is this framework uses a
220 consistent model platform to standardize both the annual index of abundance and composition data.
221 Previous standardizations of inshore surveys only standardized the index of abundance and not the age
222 compositions. Thus, the annual index is corrected for variables influencing catchability, but the age
223 compositions are not. Further, previous standardization models included environmental effects as
224 modulates of catchability. Thus, the annual index is de-trended for these variables. However, if these
225 environmental covariates affect density and not catchability, the standardization could be de-trending

226 the abundance estimates. The model platform used in this study allowed environmental covariates to
227 influence density estimates and suggests bottom temperature influences black sea bass distribution and
228 abundance.

229 Another strength of this approach is that this model can be updated for future use. It is clear that ocean
230 conditions are variable and black sea bass distribution and abundance are changing. This framework can
231 be updated with additional data and environmental covariates to quantify and account for these
232 changes in the assessment. Further, with the inclusion of wind farms in the northeast, it is likely that
233 surveys will have to change their sampling protocols and spatial footprints. The VAST models used in this
234 study can be used to make predictions in areas that can no longer be sampled.

235 The spatio-temporal models presented here integrated 10 different trawl surveys to estimate seasonal
236 changes in the distribution and abundance of the northern black sea bass stock. Results suggest that
237 black sea bass distribution and abundance are driven by bottom water temperature. The distribution of
238 black sea bass is shifting northeast and their range is expanding poleward. Relative abundance has
239 increased in the northern region (north of Hudson Canyon), while remaining relatively stable in the
240 southern region (Hudson Canyon to Cape Hatteras). Age-based estimates suggest shifts in center of
241 gravity and area occupied for all ages in the spring. The indices and age compositions created from the
242 spatio-temporal models account for these shifts and provide time series that can be directly
243 incorporated into the black sea bass stock assessment.

244

245 **References:**

246 Bell, R. J., Richardson, D. E., Hare, J. A., Lynch, P. D., & Fratantoni, P. S. (2015). Disentangling the effects
247 of climate, abundance, and size on the distribution of marine fish: an example based on four stocks from
248 the Northeast US shelf. *ICES Journal of Marine Science*, 72(5), 1311-1322.

249 Burnham, K. P., & Anderson, D. R. (2004). Multimodel inference: understanding AIC and BIC in model
250 selection. *Sociological methods & research*, 33(2), 261-304.

251 Cao, J., Thorson, J. T., Richards, R. A., & Chen, Y. (2017). Spatiotemporal index standardization improves
252 the stock assessment of northern shrimp in the Gulf of Maine. *Canadian Journal of Fisheries and Aquatic
253 Sciences*, 74(11), 1781-1793.

254 Conn, P. B. (2010). Hierarchical analysis of multiple noisy abundance indices. *Canadian Journal of
255 Fisheries and Aquatic Sciences*, 67(1), 108-120.

256 Hare JA, Morrison WE, Nelson MW, Stachura MM, Teeters EJ, Griffis RB, Alexander MA, Scott JD, Alade
257 L, Bell RJ, et al. 2016. A Vulnerability Assessment of Fish and Invertebrates to Climate Change on the
258 Northeast U.S. Continental Shelf. PLOS ONE. 11(2):e0146756.

259 Link, J.S., Nye, J.A., Hare, J.A. 2011. Guidelines for incorporating fish distribution shifts into a fisheries
260 management context. *Fish Fish*. 12:461-469.

261 Maunder, M. N., & Thorson, J. T. (2019). Modeling temporal variation in recruitment in fisheries stock
262 assessment: a review of theory and practice. *Fisheries Research*, 217, 71-86.

263 Mazur, Mackenzie D., Jerelle Jesse, Steven X. Cadrin, Samuel B. Truesdell, and Lisa Kerr. "Consequences
264 of ignoring climate impacts on New England groundfish stock assessment and management." *Fisheries
265 Research* 262 (2023): 106652.

266 Moser, J., & Shepherd, G. R. (2008). Seasonal Distribution and Movement of Black Sea Bass
267 (*Centropristis striata*) in the Northwest Atlantic as Determined from a Mark-Recapture
268 Experiment. *Journal of Northwest Atlantic Fishery Science*, 40.

269 Northeast Fisheries Science Center (NEFSC). 2017. 62nd Northeast Regional Stock Assessment Workshop
270 (62nd SAW) Assessment Report. US Dept Commer, Northeast Fish Sci Cent Ref Doc. 17-03; 822 p.
271 Available from: National Marine Fisheries Service, 166 Water Street, Woods Hole, MA 02543-1026, or
272 online at <http://www.nefsc.noaa.gov/publications/>

273 Northeast Fisheries Science Center (NEFSC). 2022. Management Track Assessment: June 2021. US Dept
274 Commer, Northeast Fish Sci Cent Ref Doc. 22-10; 79 p. <https://doi.org/10.25923/4m8f-2g46>

275 Nye, J. A., Link, J. S., Hare, J. A., & Overholtz, W. J. (2009). Changing spatial distribution of fish stocks in
276 relation to climate and population size on the Northeast United States continental shelf. *Marine Ecology
277 Progress Series*, 393, 111-129.

278 O'Leary, C. A., Thorson, J. T., Ianelli, J. N., & Kotwicky, S. (2020). Adapting to climate-driven distribution
279 shifts using model-based indices and age composition from multiple surveys in the walleye pollock
280 (*Gadus chalcogrammus*) stock assessment. *Fisheries Oceanography*, 29(6), 541-557.

281 O'Leary, C. A., DeFilippo, L. B., Thorson, J. T., Kotwicky, S., Hoff, G. R., Kulik, V. V., ... & Punt, A. E. (2022).
282 Understanding transboundary stocks' availability by combining multiple fisheries-independent surveys
283 and oceanographic conditions in spatiotemporal models. *ICES Journal of Marine Science*, 79(4), 1063-
284 1074.

285 Perretti, C. T., & Thorson, J. T. (2019). Spatio-temporal dynamics of summer flounder (*Paralichthys
286 dentatus*) on the Northeast US shelf. *Fisheries Research*, 215, 62-68.

287 Pinsky, M. L., Worm, B., Fogarty, M. J., Sarmiento, J. L., & Levin, S. A. (2013). Marine taxa track local
288 climate velocities. *Science*, 341(6151), 1239-1242.

289 Shelton, A. O., Thorson, J. T., Ward, E. J., & Feist, B. E. (2014). Spatial semiparametric models improve
290 estimates of species abundance and distribution. *Canadian Journal of Fisheries and Aquatic*
291 *Sciences*, 71(11), 1655-1666.

292 Thorson, J. T. (2019). Guidance for decisions using the Vector Autoregressive Spatio-Temporal (VAST)
293 package in stock, ecosystem, habitat and climate assessments. *Fisheries Research*, 210, 143-161.

294 Wilberg, M.J., Thorson, J.T., Linton, B.C., Berkson, J. 2010. Incorporating time-varying catchability into
295 population dynamic stock assessment models. *Rev. Fish. Sci.* 18: 7-24.

296 Zuur, A.F., Saveliev, A.A., Ieno, E.N., 2012. *Zero Inflated Models and Generalized Linear Mixed Models*
297 *with R*. Highland Statistics Ltd, Newburgh

298

299 Table 1: Summary of trawl surveys that catch black seabass in the mid-Atlantic.

Survey	Years	Months	region	Ages
Northeast Fisheries Science Center (NEFSC)	1989 – 2022	1-12	North and South	Yes
Northeast Assessment and Monitoring survey (NEAMAP)	2007 – 2022	4-6; 9_12	North and South	
Massachusetts Division of Marine Fisheries (MADMF)	1989 – 2022	4-6; 9,10	North	Yes
Rhode Island Division of Environmental Management (RIDEM)	1989 – 2022	4-6; 9-11	North	
Connecticut Department of Energy and Environmental Protection	1989 – 2022	4-6; 9-10	North	
New York Department of Environmental Conservation	1989 – 2022	4-11	North	
New Jersey Department of Environmental Protection	1989 – 2022	1-12	South	
Delaware Department of Fish and Wildlife	1989 – 2022	1-12	South	
Maryland department of Natural Resources	1989 – 2022	4-10	South	
Virginia Institute of Marine Science	1989 – 2022	1-12	South	

300

301

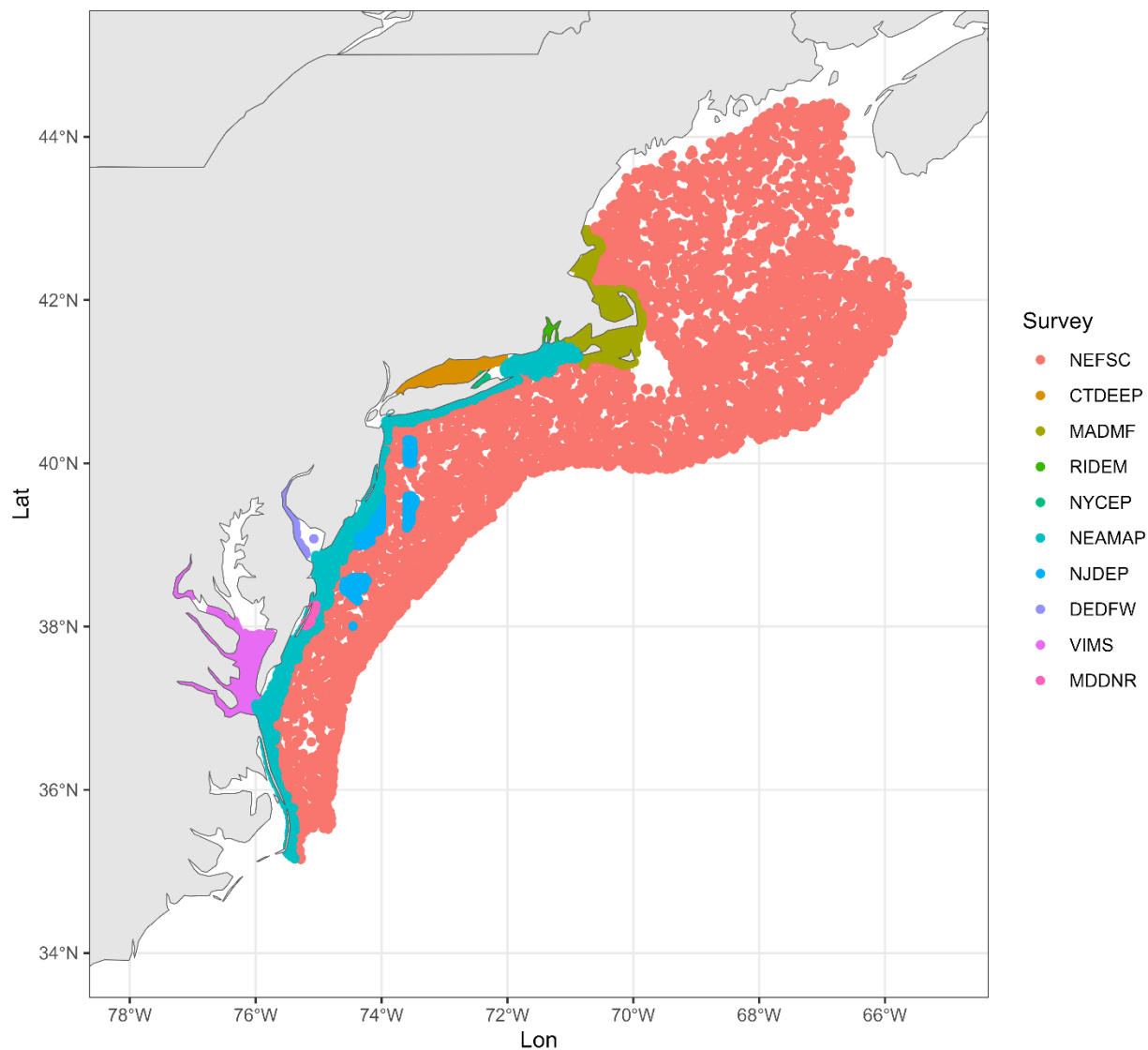
302

303 Table 2: AIC scores for VAST models.

Model	Season	Covariate	Type	AIC
Annual index	Spring	-	-	67201
		Survey	Catchability	52846
		Bottom temperature	Density	52013
		Depth	Density	52048
		Shelf water volume anomaly	Density	54031
Annual index	Fall	-	-	64801
		Survey	Catchability	54202
		Bottom temperature	Density	53308
		Depth	Density	53446
		Shelf water volume anomaly	Density	54482

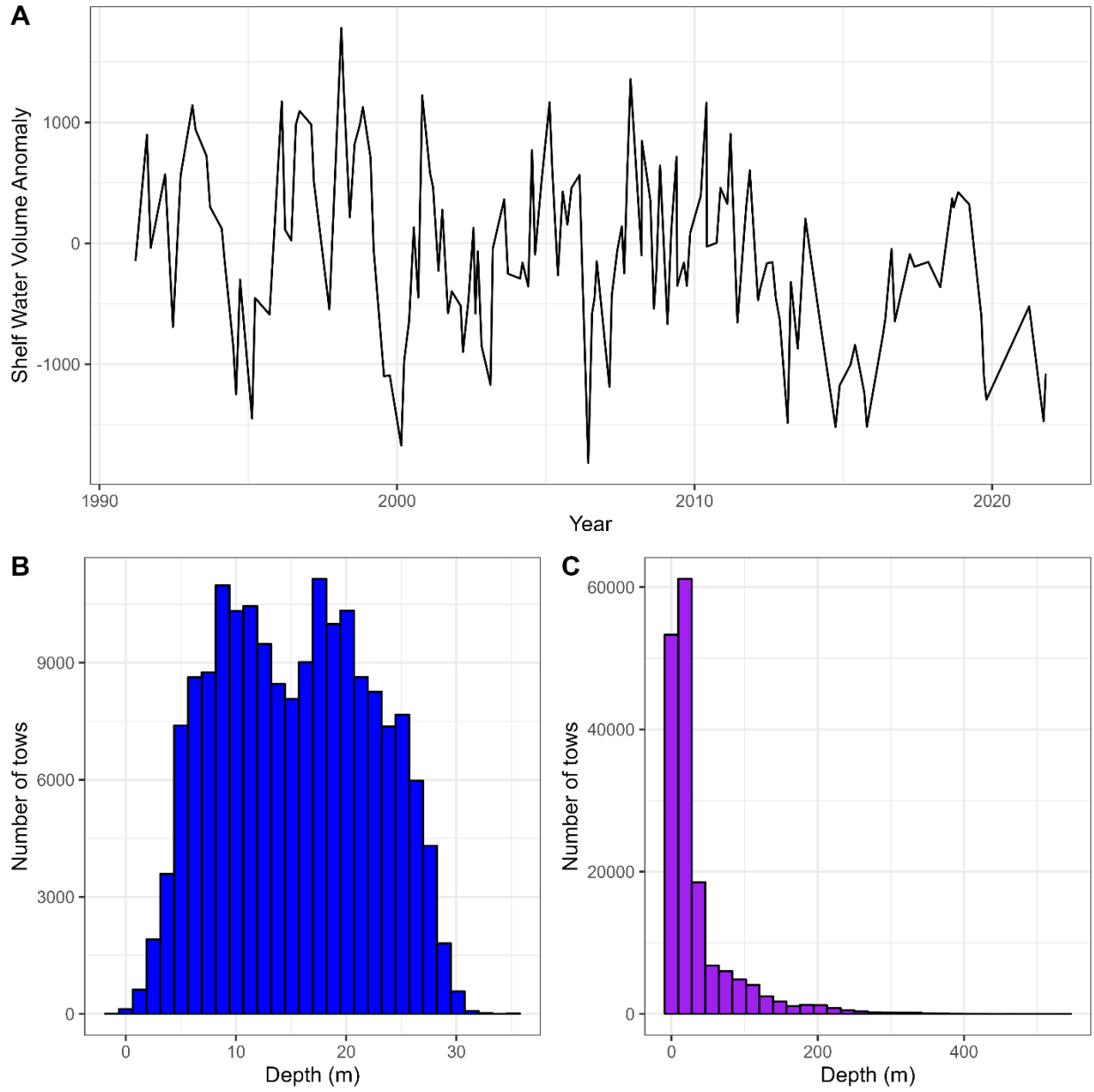
304

305



306

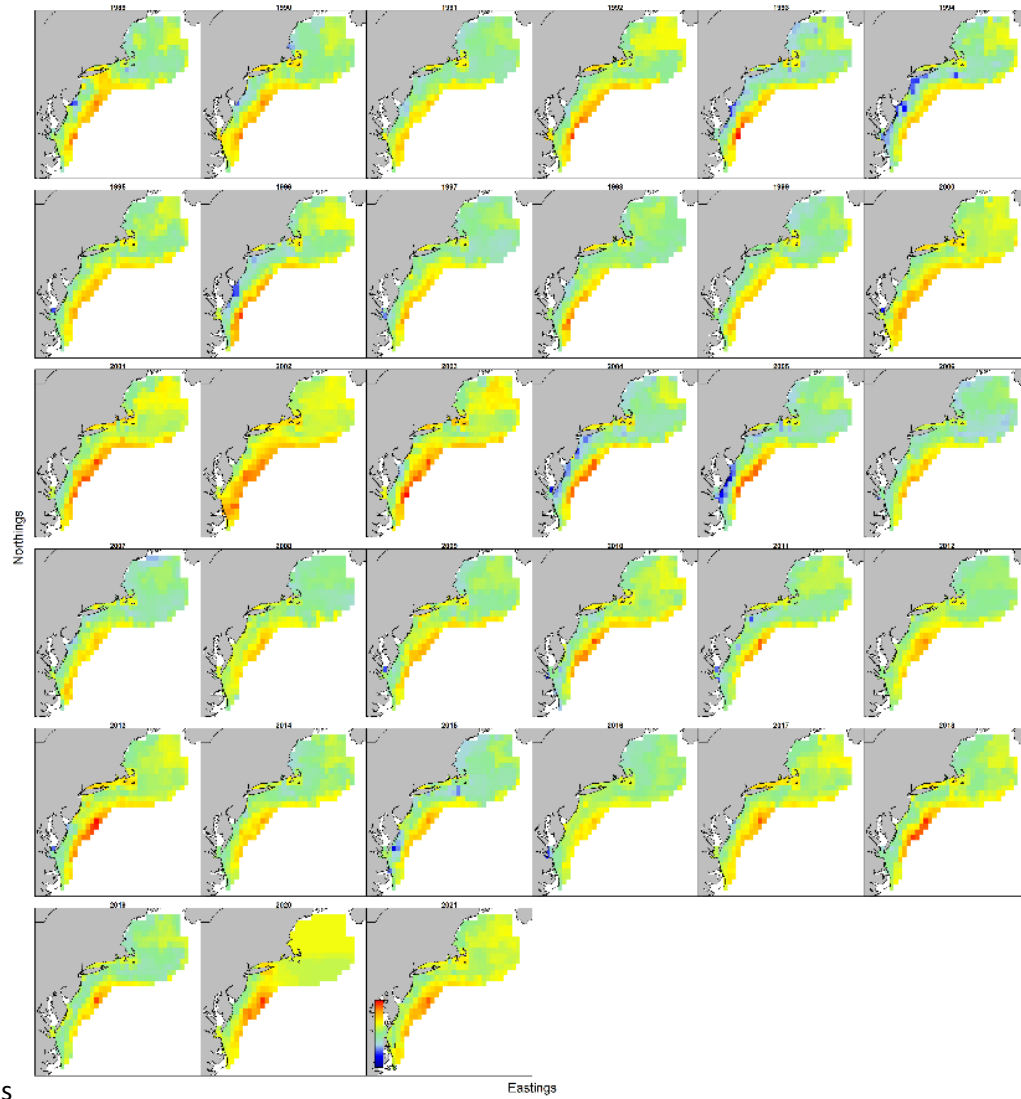
307 Figure 1: Different trawl surveys fit by VAST.



308

309 Figure 2: Covariates explored as influencing density in VAST model runs.

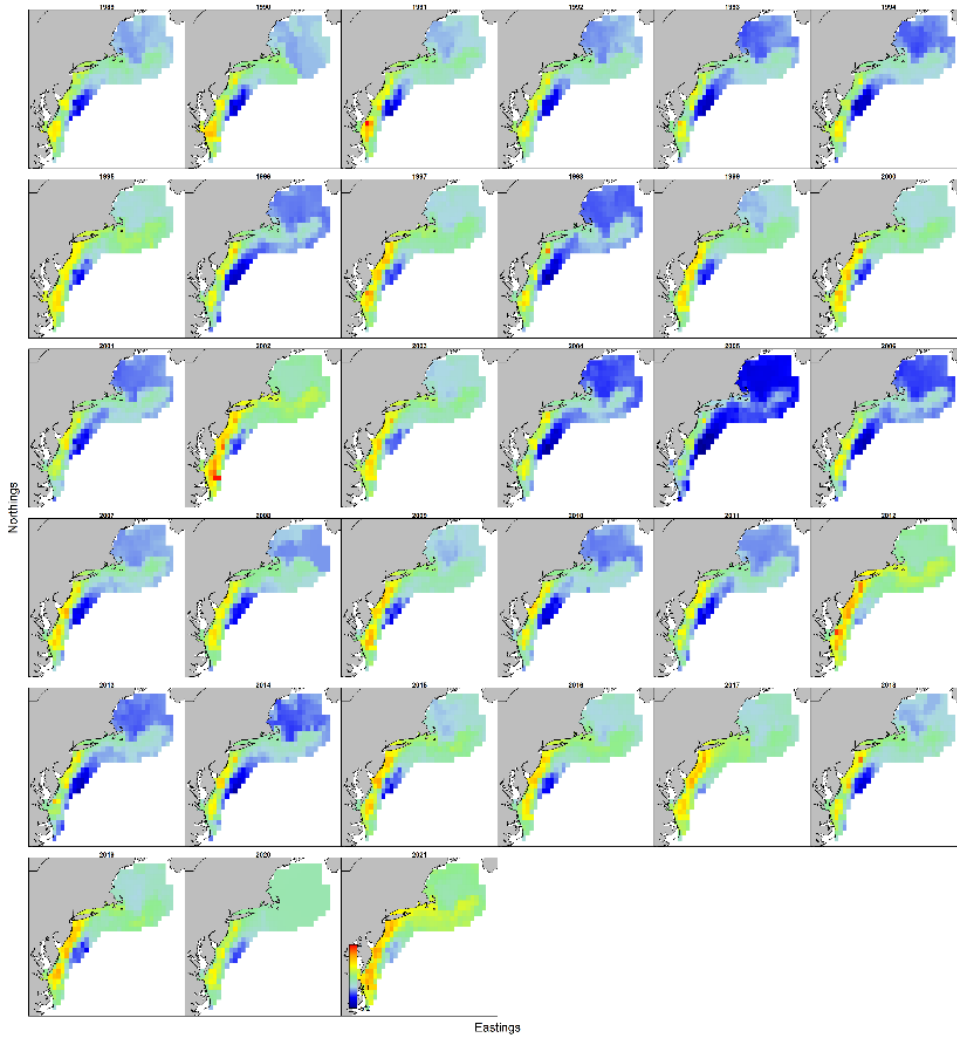
310



311 s

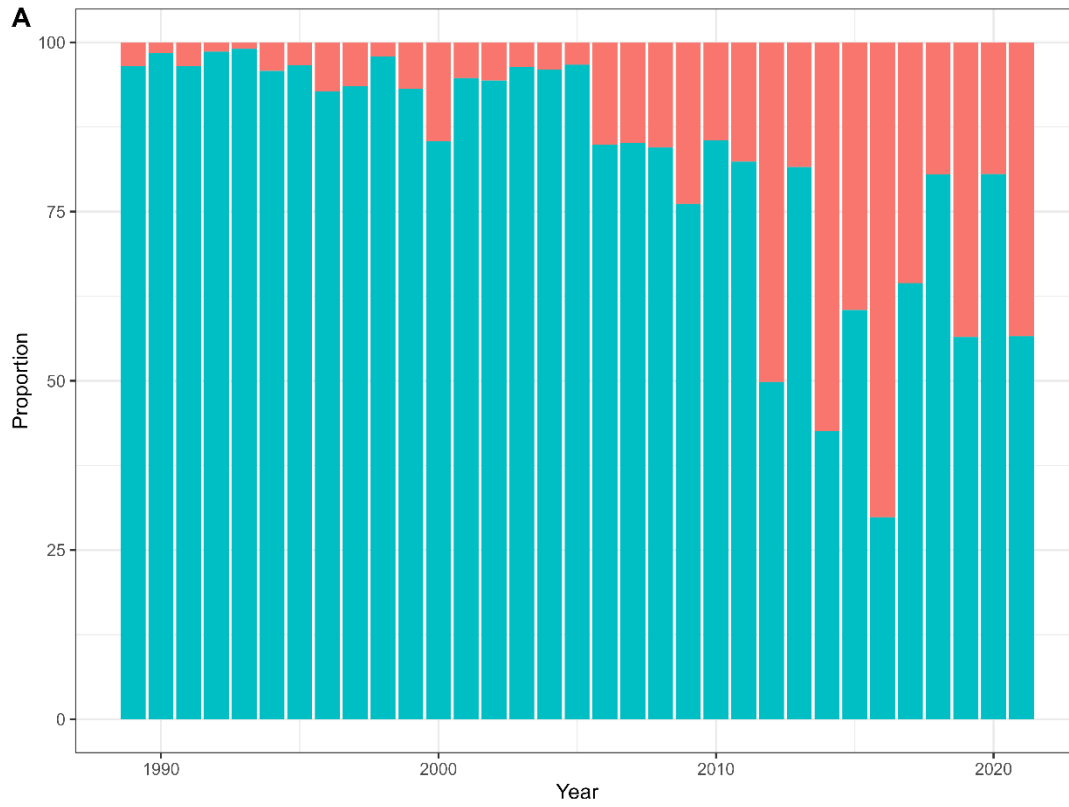
312 Figure 3: Abundance estimates produced from VAST for black sea bass in the Spring.

313



314

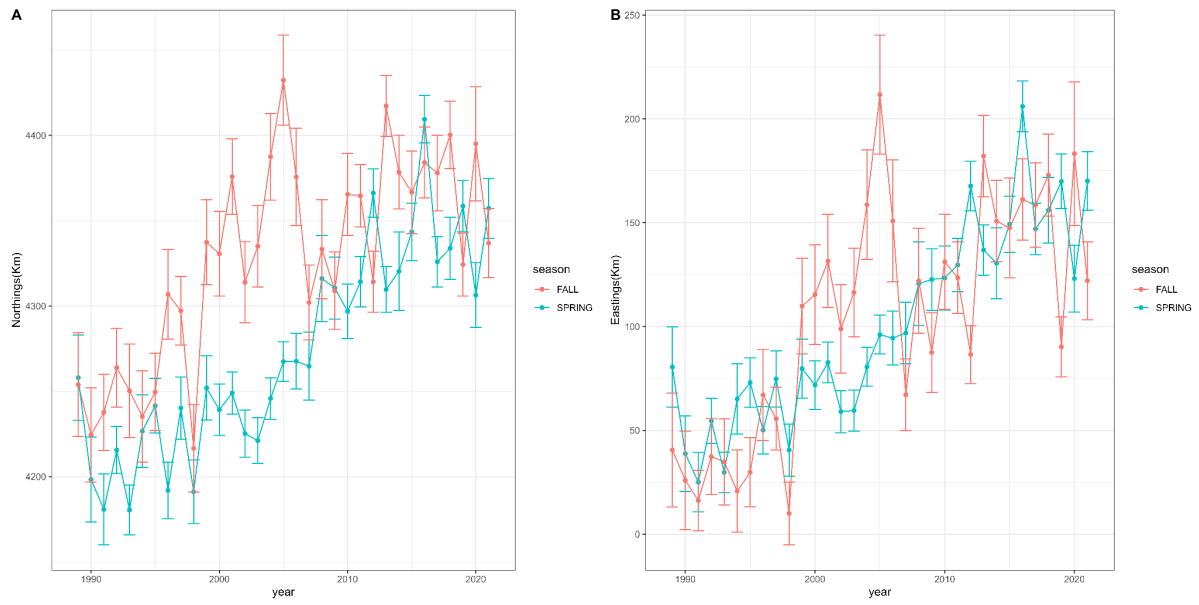
315 Figure 4: Abundance estimates produced from VAST for black sea bass in the fall.



Region ■ North ■ South

316

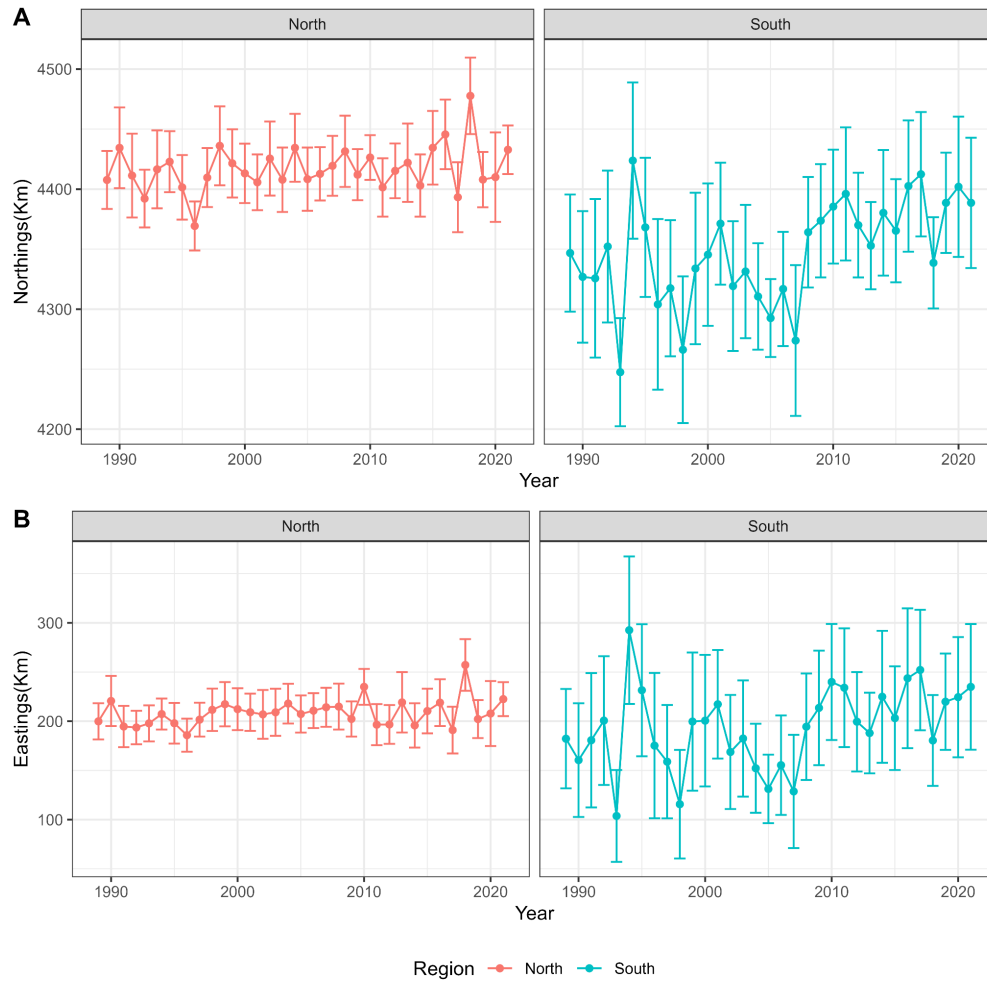
317 Figure 5: Proportion of black sea bass caught between the two regions for the spring (A) and fall (B).



318

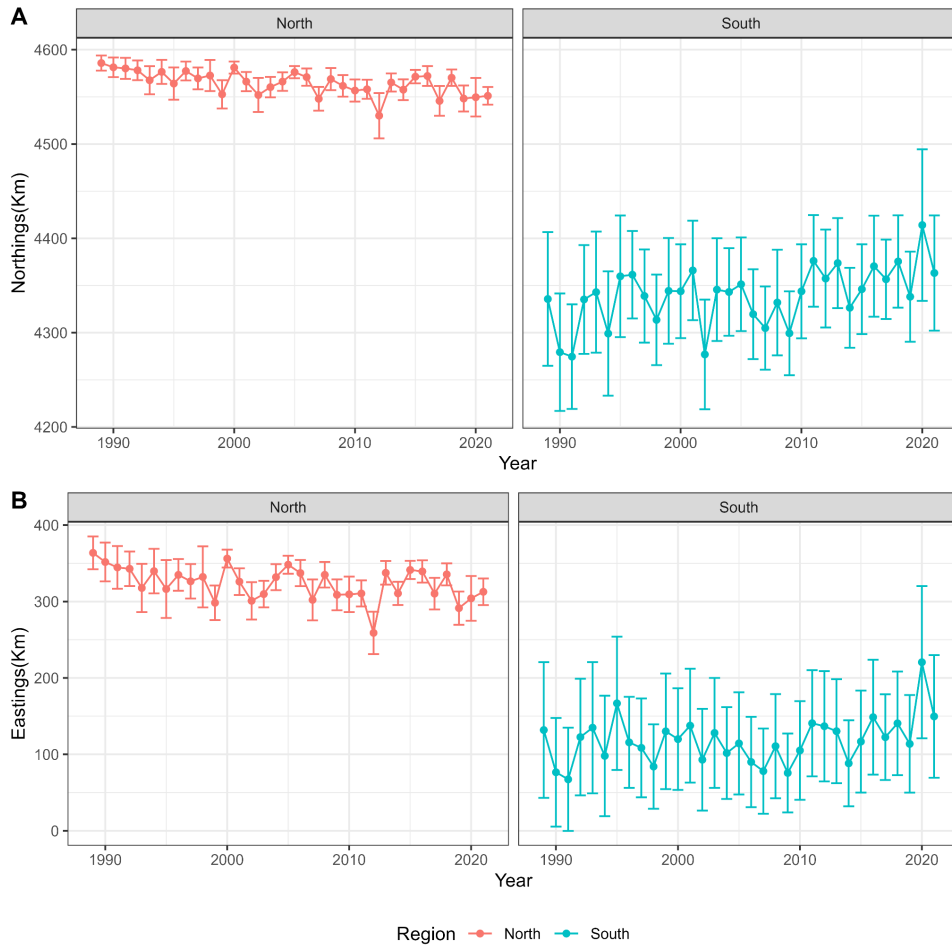
319 Figure 6: Black sea bass center of gravity estimates from VAST models for the spring and fall.

320



321

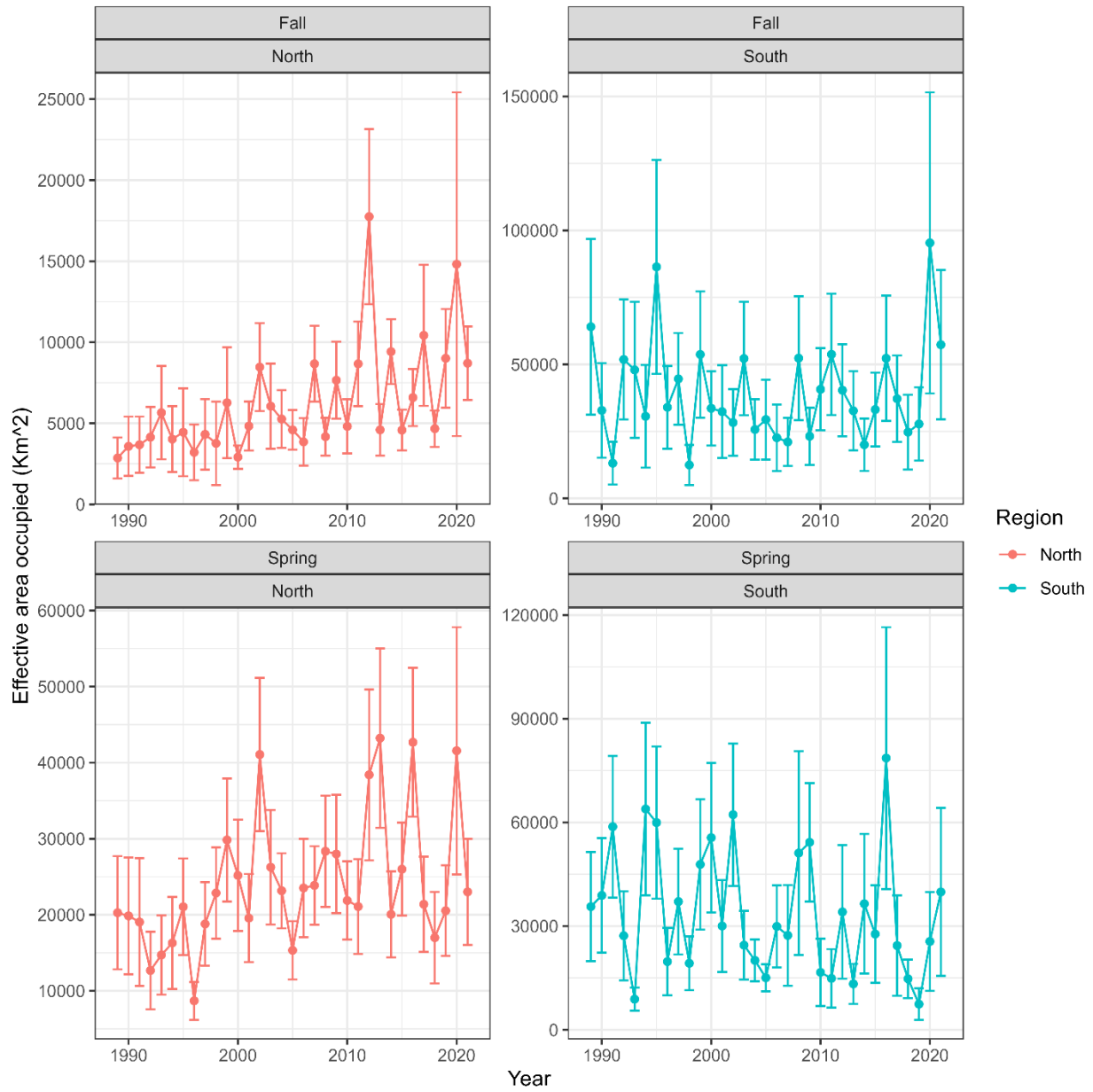
322 Figure 7: Spring center of gravity estimates from VAST for black sea bass in the north and south regions.



323

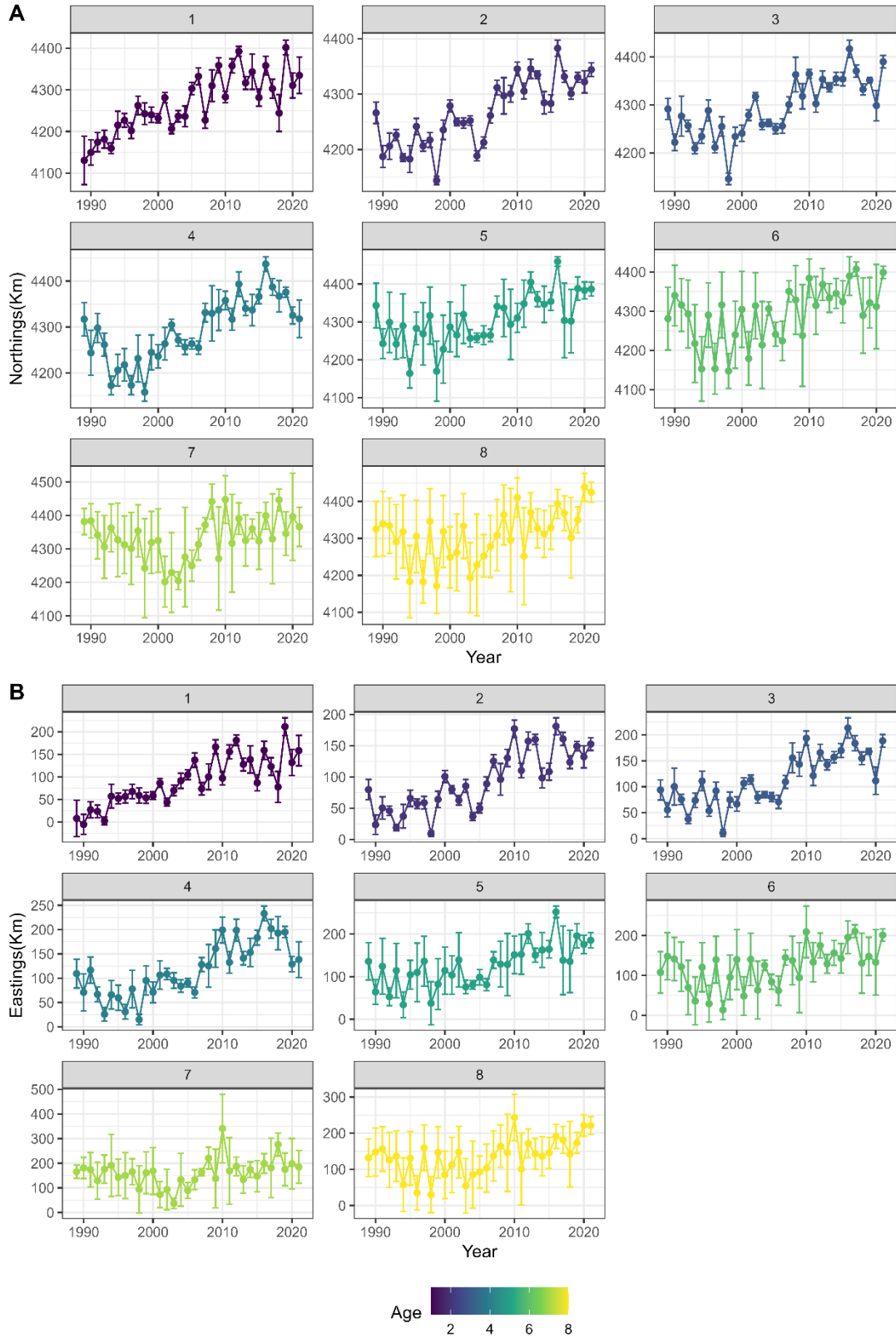
324 Figure 8: Fall center of gravity estimates from VAST for black sea bass in the north and south regions.

325



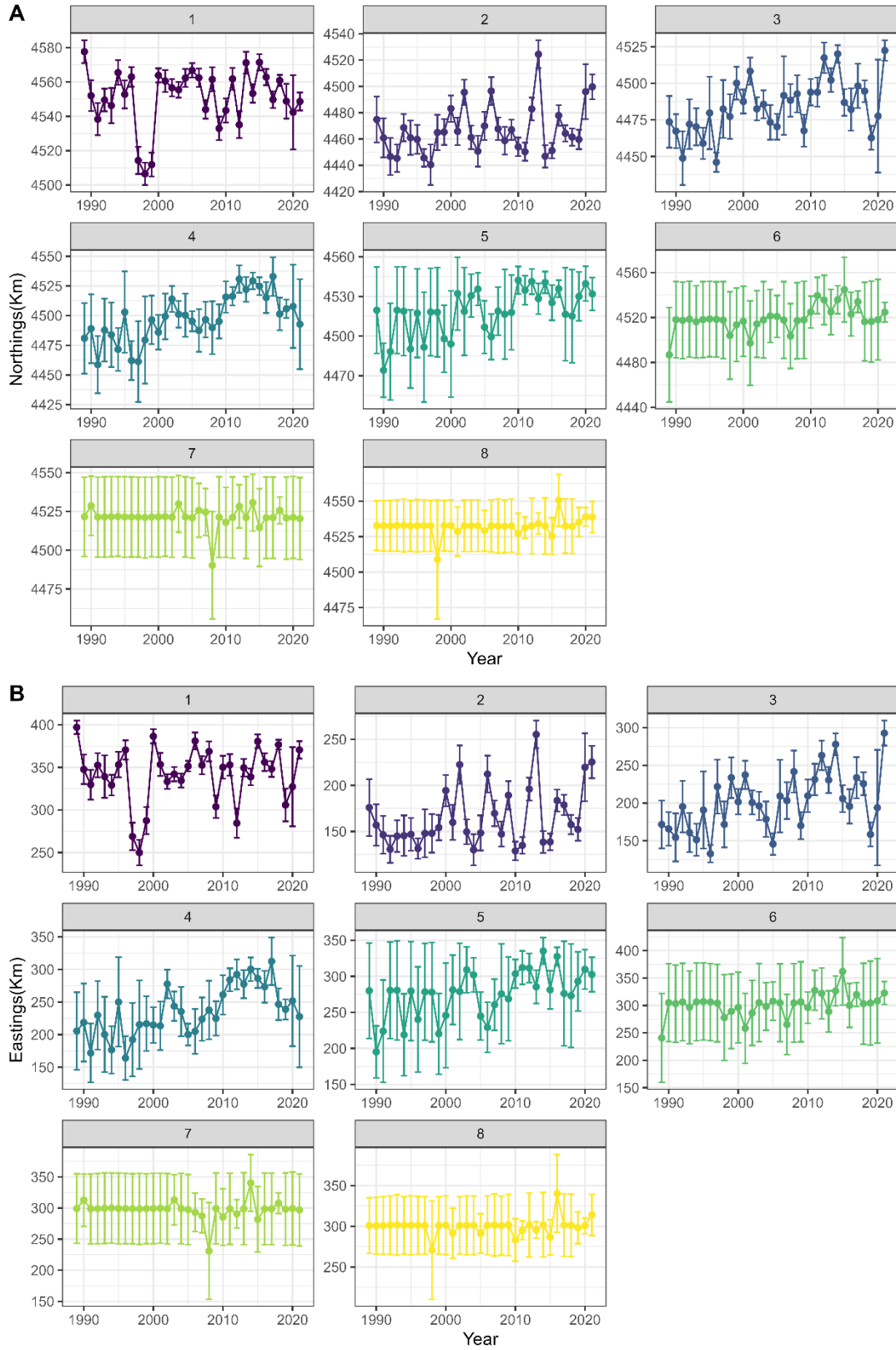
326

327 Figure 9: Effective area occupied estimates from VAST models for black sea bass for each season and
 328 region



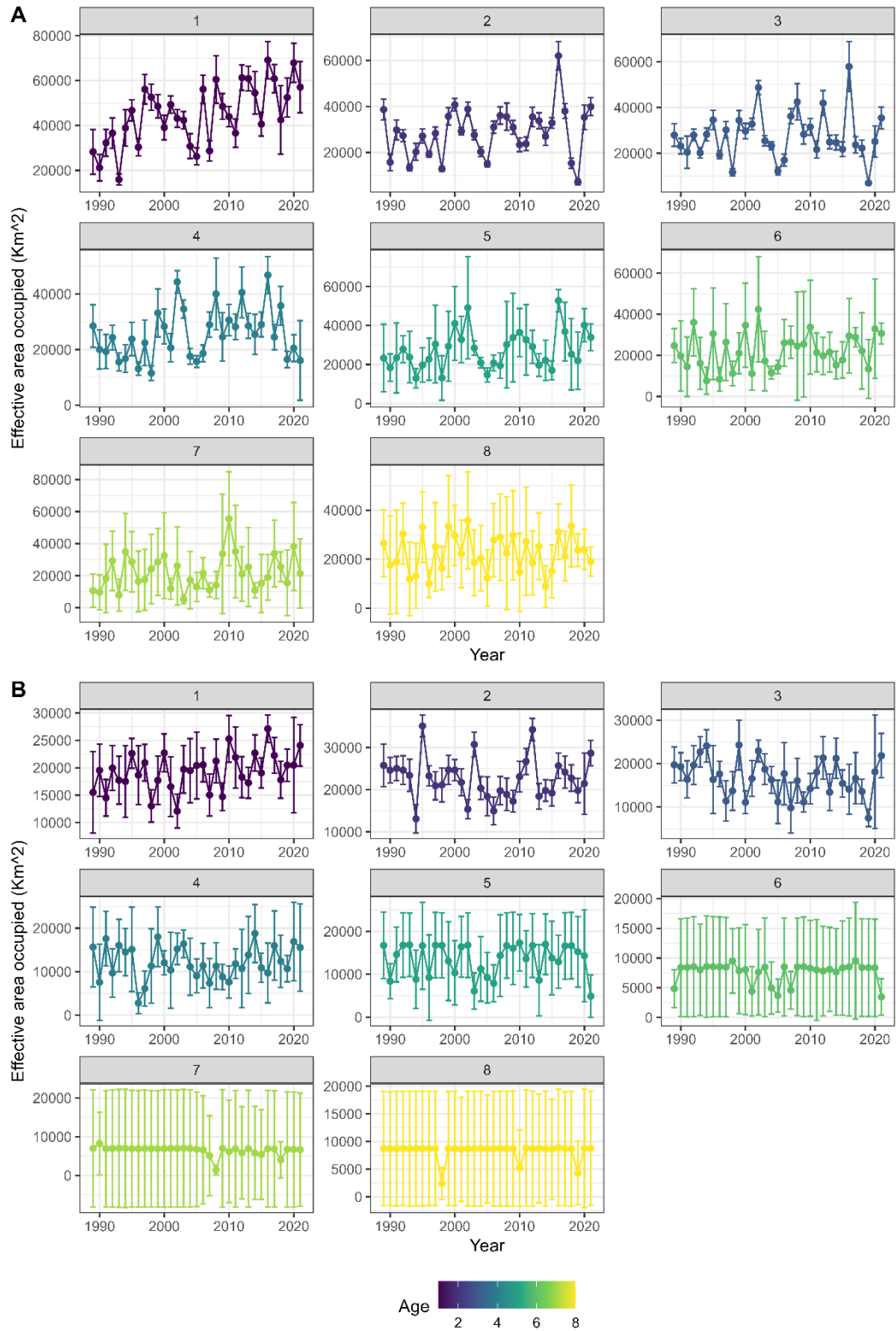
329

330 Figure 10: Age specific changes in center of gravity of black sea bass in the spring.



331

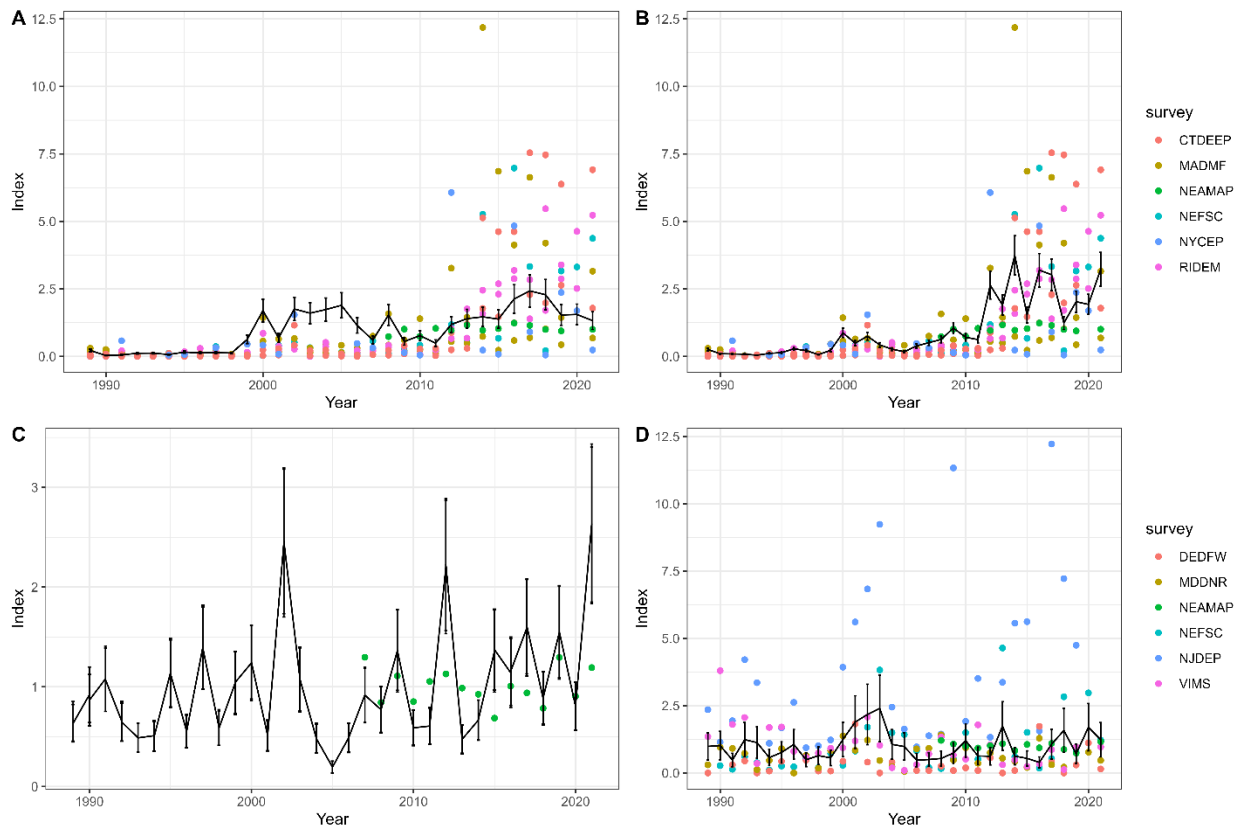
332 Figure 11: Age specific changes in center of gravity of black seas bass in the fall.



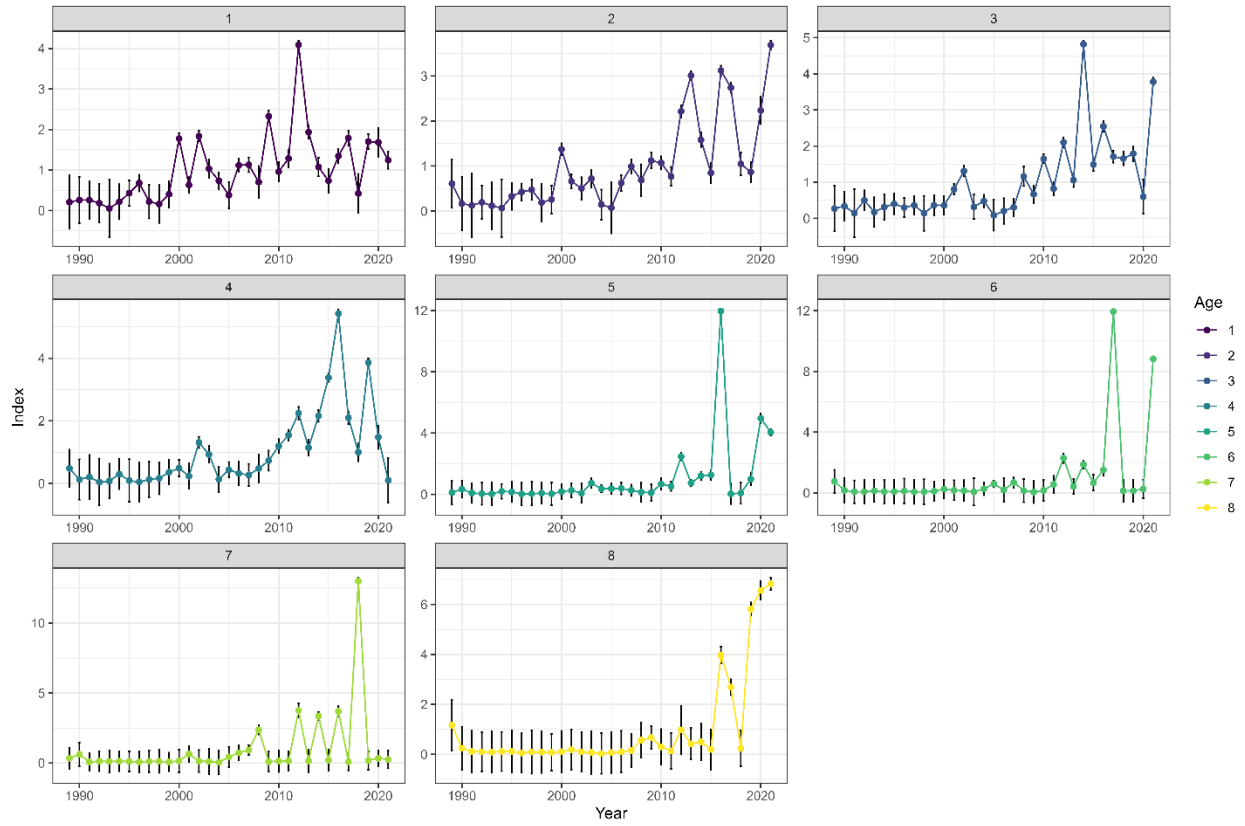
333

334 Figure 12: Age specific changes in effective area occupied of black sea bass in the spring (A) and fall (B).

335



338 Figure 13: Annual abundance indices produced by VAST (black line) and their associated CVs for the
 339 North fall and spring (A & B) as well as the South fall and spring (C & D). Colored points represent the
 340 designed based annual abundance estimates from each survey included in VAST.



341

342 Figure 14: Age based abundance estimate produced VAST for the spring.

343

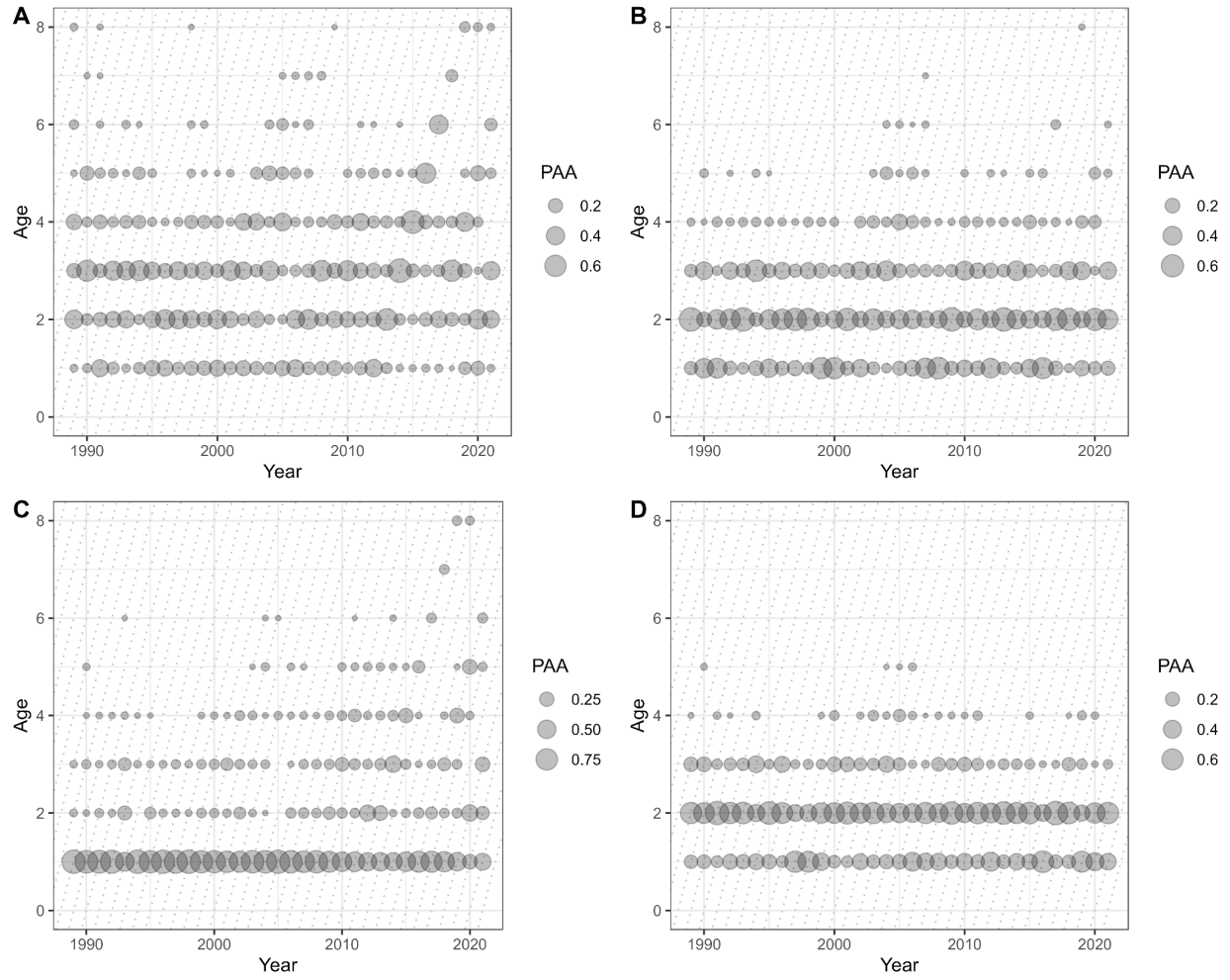


344

345

346 Figure 15: Age based abundance estimate produced VAST for the fall.

347



348

349 Figure 16: VAST age composition estimates for the northern region (A) and southern region (B) in the
 350 spring. VAST age composition estimates for the northern (C) and southern region in the fall (D).